The effect of rotation on the Rayleigh-Bénard stability threshold

Andrea Prosperetti[a)]
Department of Mechanical Engineering, Johns Hopkins University, Baltimore, Maryland 21218, USA

(Received 12 April 2012; accepted 24 September 2012; published online 26 November 2012)

The standard method used to solve the Rayleigh-Bénard linear stability problem for a rotating fluid leads to a complex expression which can only be evaluated numerically. Here the problem is solved by a different method similar to that used in a recent paper on the non-rotating case [A. Prosperetti, "A simple analytic approximation to the Rayleigh-Bénard stability threshold," Phys. Fluids **23**, 124101 (2011)]. In principle the method leads to an exact result which is not simpler than the standard one. Its value lies in the fact that it is possible to obtain from it an approximate explicit analytic expression for the dependence of the Rayleigh number on the wave number of the perturbation and the rate of rotation at marginal stability conditions. Where the error can be compared with exact results in the literature, it is found not to exceed a few percent over a very broad Taylor number range. The relative simplicity of the approach permits us, among others, to account for the effects of a finite thermal conductivity of the plates, which have not been studied before. © *2012 American Institute of Physics*. [http://dx.doi.org/10.1063/1.4764931]

I. INTRODUCTION

The stabilizing effect of rotation on an unstably thermally stratified fluid layer is a well-known feature of this so-called Rayleigh-Bénard problem, first studied in detail by Chandrasekhar[1] and by several other authors after him. Chandrasekhar summarized the earlier results in his 1961 monograph[2] with a special emphasis on the case in which the parallel plates bounding the infinite fluid layer allow a free slip of the fluid. The more realistic case of no-slip plates is algebraically much more involved and Chandrasekhar only presented approximate numerical results for the minimum of the Rayleigh number vs. wave number relation for several values of the rotation rate.[1,2] He argued that the precise nature of the boundary conditions on the plates is immaterial for very rapid rotation.

This observation was subsequently confirmed in Ref. 3, where it was shown that, in a rapidly rotating fluid, viscous effects are limited to thin Ekman layers with a dimensionless thickness scaling as $Ta^{-1/3}$ for free-slip and as $Ta^{-1/12}$ for no-slip boundaries. Here $Ta = 4\Omega^2 H^4/\nu^2$ is the Taylor number (essentially the square of the ratio of the Coriolis and viscous forces), with Ω the angular velocity of rotation, H the plate separation, and ν the kinematic viscosity of the fluid. For large Ta, therefore, the bulk of the motion is close to inviscid and free-slip conditions would be appropriate. There are some subtleties here as the Proudman-Taylor theorem would make an inviscid fluid stable. What happens is that viscosity has a subtle destabilizing effect by progressively reducing the horizontal scale of the motion for large Ta,[3–5] but this feature does not affect the basic conclusion as to the insensitivity of the result to the precise nature of the boundary conditions.

In the rotating free-slip case, when the Prandtl number of the fluid is smaller than about 0.67659, the instability sets in as an oscillatory Hopf bifurcation at a Prandtl-number-dependent critical value of the Rayleigh number.[2,6] Many features of this oscillatory onset and its

[a)] Also at Faculty of Science and Technology and J. M. Burgers Center for Fluid Dynamics, University of Twente, 7500AE Enschede, The Netherlands. Electronic mail: prosperetti@jhu.edu.

finite-amplitude development have been extensively studied (see, e.g., Refs. 5 and 7–9). For larger values of the Prandtl number, the onset of the instability is non-oscillatory and independent of the Prandtl number. Finlayson[10] showed that the same numerical estimate of the transition Prandtl number holds, if somewhat less accurately, for the no-slip case when the plates have infinite thermal conductivity.

In this paper we use the same method developed in a recent study of the non-rotating linear stability problem[11] to determine an approximate solution for a rotating, laterally infinite fluid layer. The rotation axis is parallel to gravity and perpendicular to the no-slip plates bounding the fluid. We focus on the marginal stability conditions for Prandtl numbers large enough that the instability is non-oscillatory. Our approach appears suitable for the Hopf bifurcation case as well, but at the expense of a greater amount of algebra. As for the limitation inherent in the analysis of a laterally unbounded fluid layer, it may be mentioned that, as shown in Ref. 4, the results for bounded fluid layers are similar in many respects to those for unbounded layers.

Over a large range of Taylor numbers, our approximate solution matches within a few percent the numerical values provided by earlier investigators for the minimum, or critical, value Ra_c of the Rayleigh number and the corresponding wave number k_c. While less accurate than some available numerical results, a major advantage of the solution developed here lies in its explicit form which makes it relatively straightforward to generate complete curves $Ra(k; Ta)$ of the Rayleigh number vs. the wave number and to explore other effects not hitherto studied, such as a finite thermal conductivity of the plates.

As in all the earlier work devoted to the linear stability problem, we study the normal modes of the system at conditions of marginal stability. Our approach is based on the use of a Fourier series expansion which, unlike other investigations (e.g., Refs. 12 and 13), is never differentiated. This feature provides for a much faster convergence and, in fact, our results are obtained by simply truncating the series to its first term.

To be sure, most of the interest in the Rayleigh-Bénard problem centers on nonlinear effects (see, e.g., the reviews provided in Refs. 14–16) rather than the linear problem studied here. Nevertheless, the availability of an explicit approximate solution may be used to develop analytically tractable weakly nonlinear theories as well as to study aspects of the instability that have not been investigated before.

Algebraic details of the derivation are briefly covered in Appendix A and, more extensively, in the supplementary material.[17] Appendix B summarizes the conventional approach to the problem and extends it to modes with an odd parity about the center plane of the cell.

II. MATHEMATICAL FORMULATION

We consider a Boussinesq fluid contained between two infinitely extended plates normal to the direction of gravity separated by a distance H. In undisturbed conditions the fluid and the plates are in solid body rotation with an angular velocity Ω around an axis parallel to gravity and perpendicular the plates. Since the mathematical framework of the linear problem is well known, we can omit details and start from the set of dimensionless equations derived by Chandrasekhar,[2] namely

$$(\partial_z^2 - k^2)T' = -Pr\, u_z', \tag{1}$$

$$(\partial_z^2 - k^2)\omega_z' = -\sqrt{Ta}\,\partial_z u_z', \tag{2}$$

$$(\partial_z^2 - k^2)^2 u_z' - \frac{Ra}{Pr}k^2 T' - \sqrt{Ta}\,\partial_z \omega_z' = 0. \tag{3}$$

Here the dimensionless perturbation temperature, vertical vorticity and velocity have been written, respectively, as

$$T'(z)\, f_k(x, y), \qquad \omega_z'(z)\, f_k(x, y), \qquad u_z'(z)\, f_k(x, y) \tag{4}$$

with $\nabla^2 f_k = -k^2 f_k$ and k a dimensionless wave number. The symbol ∂_z denotes differentiation in the vertical direction z. Equation (1) is the energy equation, (2) is the vertical vorticity equation, and (3) is obtained by taking the double curl of the momentum equation in the z-direction.

The Rayleigh Ra, Prandtl Pr, and Taylor Ta numbers have their usual definitions:

$$Ra = \frac{\beta g H^3 (T_H - T_C)}{\nu D}, \qquad Pr = \frac{\nu}{D}, \qquad Ta = \frac{4\Omega^2 H^4}{\nu^2} \tag{5}$$

with β the coefficient of thermal expansion, g the acceleration of gravity, H the plate separation, $T_H - T_C$ the difference between the undisturbed temperatures of the lower, warmer plate and that of the upper, colder plate, ν the kinematic viscosity, D the thermal diffusivity, and Ω the angular velocity of rotation. The equations have been non-dimensionalized in terms of H for length, H^2/ν for time, and $T_H - T_C$ for temperature. Time derivatives have been omitted in keeping with our focus on the marginal stability conditions for conditions in which the principle of exchange of stabilities holds.[2]

We take $z = 0$ on the midplane between the two plates so that the fluid layer extends in the region $-\frac{1}{2} < z < \frac{1}{2}$. For simplicity the thickness of the both plates is assumed to be infinite, extending between $\pm\frac{1}{2}$ and $\pm\infty$. Since the range of (dimensionless) wave numbers of interest in practice is of order unity, one may expect that plates with a thickness comparable to, or greater than, the liquid layer would essentially behave as semi-infinite. This has indeed been proven in the non-rotating case.[18]

In order to account for the finite thermal conductivity of the upper plate, which occupies the region $z \geq \frac{1}{2}$, we write the (dimensional) temperature distribution T_u within it as

$$\frac{T_u - T_C}{T_H - T_C} = -\kappa_u \left(z - \frac{1}{2}\right) + T_u'(z) f_k(x, y), \tag{6}$$

in which $\kappa_u = K/K_u$ is the ratio of the thermal conductivities of the fluid, K, and of the upper plate, K_u, and T_u' is the dimensionless temperature perturbation in the plate. As written, the first term in the right-hand side ensures the continuity of temperature and heat flux at the plate surface in undisturbed conditions. We use a similar representation for the lower plate temperature distribution in the region $z \leq -\frac{1}{2}$,

$$\frac{T_l - T_H}{T_H - T_C} = -\kappa_l \left(z + \frac{1}{2}\right) + T_l'(z) f_k(x, y) \tag{7}$$

with $\kappa_l = K_l/K$. The temperature perturbations in the plates satisfy an energy equation which, for marginal conditions, reduces to the form

$$\left(\partial_z^2 - k^2\right) T_{l,u}' = 0. \tag{8}$$

Thus,

$$T_l' = T'(z = -1/2)\, e^{k(z+1/2)}, \qquad T_u' = T'(z = 1/2)\, e^{-k(z-1/2)}, \tag{9}$$

in which $T'(z = \pm 1/2)$ denote the temperature perturbations at the hot and cold plates, common to fluid and plates by continuity of the temperature. With these solutions, the requirement of continuity of the heat fluxes at the plate surfaces can be expressed solely in terms of the temperature perturbation T' in the fluid and is given by[19]

$$\left[k\kappa_l T' - \partial_z T'\right]_{z=-1/2} = 0, \qquad \left[k\kappa_u T' + \partial_z T'\right]_{z=1/2} = 0. \tag{10}$$

While in most of the analysis we give results for arbitrary κ_l and κ_u, for simplicity numerical results will only be presented for $\kappa_l = \kappa_u$.

The other boundary conditions are the vanishing of u_z' and $\partial_z u_z'$ on the plates, the latter requirement a consequence of the equation of continuity coupled with the no-slip condition. Finally, and again because of the no-slip condition, the vorticity ω_z' must also vanish on the plates.

III. SOLUTION

Upon applying the operator $\partial_z^2 - k^2$ to (3) and using (1) and (2) to eliminate T' and ω_z', we find an equation that may be written as

$$(\partial_z^2 - k^2)[(\partial_z^2 - k^2)^2 + Ta]u_z' = -(Ra + Ta)k^2 u_z'. \tag{11}$$

The absence of the Prandtl number from this equation is a consequence of the present focus on the non-oscillatory transition to instability. We now expand u_z' into a complete set of orthogonal functions as

$$u_z' = \sum_{n=1}^{\infty} \left[U_n \sin 2n\pi z + \tilde{U}_n \cos(2n-1)\pi z \right]. \tag{12}$$

Here and in the following a tilde is consistently used to denote quantities pertaining to the modes symmetric about the midplane $z = 0$. As will be seen later, for situations in which the modes have a definite parity, the first mode of this family is the one which becomes unstable first.

The expansion (12) is substituted in the right-hand side of (11) and the equation is solved for $(\partial_z^2 - k^2)^2 u_z' + Ta\, u_z'$ to find

$$(\partial_z^2 - k^2)^2 u_z' + Ta\, u_z' = (Ra + Ta)k^2 \sum_{n=1}^{\infty} \left(\frac{U_n}{\Delta_n} \sin 2n\pi z + \frac{\tilde{U}_n}{\tilde{\Delta}_n} \cos(2n-1)\pi z \right) + W_c F_c(z) + W_s F_s(z), \tag{13}$$

in which $W_{c,s}$ are integration constants and

$$\Delta_n = 4\pi^2 n^2 + k^2, \qquad \tilde{\Delta}_n = (2n-1)^2 \pi^2 + k^2. \tag{14}$$

The solutions of the homogeneous equation $(\partial_z^2 - k^2)F_{c,s} = 0$ have been denoted by

$$F_c(z) = \cosh kz, \qquad F_s(z) = \sinh kz. \tag{15}$$

Earlier investigators who made use of a Fourier series representation of the velocity similar to (12) substituted it into the field equations.[12,13] The necessary differentiations decrease or may even impair the convergence properties of the series. Our approach is instead to integrate the Fourier series, as in the step from (11) to (13), which greatly benefits the rate of convergence, so much so, in fact, that truncation to just the first term produces reasonably accurate results as will be shown later.

The term $Ta\, u_z'$ in the left-hand side of (13) may be taken to the other side and incorporated into the summation after using (12) to express u_z'. The resulting equation for u_z' can then be solved with the result

$$u_z' = \sum_{n=1}^{\infty} \left[\left(\frac{(Ra + Ta)k^2}{\Delta_n} - Ta \right) U_n \frac{\sin 2n\pi z}{\Delta_n^2} + \left(\frac{(Ra + Ta)k^2}{\tilde{\Delta}_n} - Ta \right) \tilde{U}_n \frac{\cos(2n-1)\pi z}{\tilde{\Delta}_n^2} \right] + W_c H_c + W_s H_s + V_c G_c + V_s G_s + U_c F_c + U_s F_s, \tag{16}$$

in which $V_{c,s}$ and $U_{c,s}$ are additional integration constants, and $G_{c,s}$ and $H_{c,s}$, explicitly given in (A1) and (A2), solve the equations $(\partial_z^2 - k^2)G_{c,s} = F_{c,s}$ and $(\partial_z^2 - k^2)H_{c,s} = G_{c,s}$.

By imposing that $u_z' = 0$ and $\partial_z u_z' = 0$ at $z = \pm\frac{1}{2}$ we can express $V_{c,s}$ and $U_{c,s}$ in terms of $W_{c,s}$; the results are shown in (A3)–(A6) in Appendix A. The remaining integration constants $W_{c,s}$ are determined by imposing that (3) be satisfied at the plate surfaces as shown later.

We can now take the scalar product of (16) by $\sin 2n\pi z$ to find

$$\left[1 - \frac{1}{\Delta_n^2} \left(\frac{(Ra + Ta)k^2}{\Delta_n} - Ta \right) \right] U_n = \left[I_n^H + I_n^G \frac{V_s}{W_s} + I_n^F \frac{U_s}{W_s} \right] W_s, \tag{17}$$

while the scalar product with $\cos(2n-1)\pi z$ gives

$$\left[1 - \frac{1}{\tilde{\Delta}_n^2} \left(\frac{(Ra + Ta)k^2}{\tilde{\Delta}_n} - Ta \right) \right] \tilde{U}_n = \left[\tilde{I}_n^H + \tilde{I}_n^G \frac{V_c}{W_c} + \tilde{I}_n^F \frac{U_c}{W_c} \right] W_c, \tag{18}$$

in which

$$I_n^F = 2\int_{-1/2}^{1/2} \sin 2n\pi z\, F_s(z)\, dz, \qquad \tilde{I}_n^F = 2\int_{-1/2}^{1/2} \cos(2n-1)\pi z\, F_c(z)\, dz, \tag{19}$$

$I_n^{G,H}$ and $\tilde{I}_n^{G,H}$ are given by similar expressions with $F_{c,s}$ replaced by $G_{c,s}$ and $H_{c,s}$. When $W_{c,s}$ are expressed in terms of the U_n and $\tilde{U}_n$, (17) and (18) constitute a linear homogeneous system the solvability condition of which determines the relation between Ra, Ta and k which expresses the marginal stability condition.

The necessary steps are straightforward but tedious and are summarized in Appendix A. A more detailed electronic document is also available.[17] Here we simply show the results which may be written as

$$\left[1 - \frac{1}{\Delta_n^2}\left(\frac{(Ra+Ta)k^2}{\Delta_n} - Ta\right)\right] U_n = Ta\sum_{m=1}^{\infty} B_{nm}(k)U_m - Ra\sum_{m=1}^{\infty} A_{nm}(k,\kappa)U_m \tag{20}$$

and

$$\left[1 - \frac{1}{\tilde{\Delta}_n^2}\left(\frac{(Ra+Ta)k^2}{\tilde{\Delta}_n} - Ta\right)\right] \tilde{U}_n = Ta\sum_{m=1}^{\infty} \tilde{B}_{nm}(k)\tilde{U}_m - Ra\sum_{m=1}^{\infty} \tilde{A}_{nm}(k,\kappa)\tilde{U}_m, \tag{21}$$

in which $A_{nm}(k, \kappa)$, $B_{nm}(k)$, etc., are given in (A18)–(A23) of Appendix A. For fixed m and $n \gg k$ all of these coefficients decay proportionally n^{-3} suggesting a fast convergence of the series.

It may be noted that the coefficients U_n of the odd modes are not coupled to the coefficients $\tilde{U}_n$ of the even modes because we have assumed for simplicity—and will continue to assume henceforth—that the thermal conductivities of the plates are equal so that $\kappa_l = \kappa_u = \kappa$. For $Ta = 0$, (20) and (21) coincide with the results of Ref. 11 which were derived in a slightly different way.

IV. ONE-TERM TRUNCATION

Upon retaining only the terms with $n = m = 1$ in (20) and (21) we are left with

$$\left[1 + \left(A_{11} - \frac{k^2}{\Delta_1^3}\right) Ra + \left(\frac{4\pi^2}{\Delta_1^3} - B_{11}\right) Ta\right] U_1 = 0 \tag{22}$$

and

$$\left[1 + \left(\tilde{A}_{11} - \frac{k^2}{\tilde{\Delta}_1^3}\right) Ra + \left(\frac{\pi^2}{\tilde{\Delta}_1^3} - \tilde{B}_{11}\right) Ta\right] \tilde{U}_1 = 0. \tag{23}$$

The vanishing of the quantities in brackets gives the desired approximations to the marginal stability relations,

$$\left(\frac{k^2}{\Delta_1^3} - A_{11}\right) Ra = 1 + \left(\frac{4\pi^2}{\Delta_1^3} - B_{11}\right) Ta \tag{24}$$

and

$$\left(\frac{k^2}{\tilde{\Delta}_1^3} - \tilde{A}_{11}\right) Ra = 1 + \left(\frac{\pi^2}{\tilde{\Delta}_1^3} - \tilde{B}_{11}\right) Ta. \tag{25}$$

Just as in the non-rotating case, it is found that the stability threshold (25) for the even modes is lower than the threshold (24) for the odd modes.

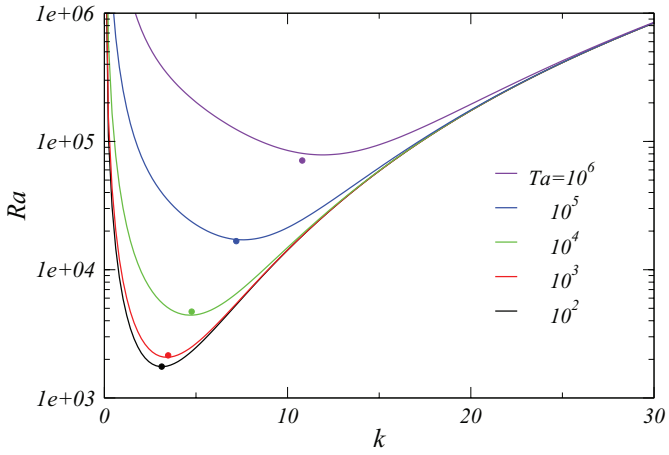

FIG. 1. The Rayleigh number for the neutral stability of the even modes with no-slip plates at fixed temperatures (i.e., $\kappa \to \infty$) as given by the present solution truncated to the first term of the Fourier expansion. In ascending order $Ta = 10^2$, 10^3, 10^4, 10^5, and 10^6. The circles mark the position of the minimum according to the numerical evaluation of the exact expression (B7).

V. EVEN MODES

The only case that appears to have been studied before is for constant plate surface temperature, which is contained in our results by taking the limit $\kappa \to \infty$. In this case the expressions (A22) and (A23) of Appendix A for the coefficients $\tilde{A}_{11}$ and $\tilde{B}_{11}$ simplify to

$$\tilde{A}_{11} = \frac{8\pi^2 k^3(\cosh k + 1)}{(k^2 + \pi^2)^5(k + \sinh k)}, \tag{26}$$

TABLE I. The smallest Rayleigh number and corresponding dimensionless wave number for the marginal stability threshold of the even modes as functions of the Taylor number, shown in the first column. The no-slip condition is applied at the plates, which are assumed to be infinitely conducting so that $\kappa \to \infty$ and their temperatures is fixed. The second and third columns show the results of the present numerical evaluation of the exact expression (B7), which are also marked by circles in Figure 1. The fourth and fifth columns reproduce the results of Ref. 2 obtained from a second-order variational approximation. The sixth and seventh columns are from the present Fourier series solution truncated to one term, Eq. (25), and the eighth and ninth from a truncation to two terms. In the latter case, the present method also gives a result for the next mode which is shown in the last two columns.

	Numerical (B7)		Ref. 2		Approximate, 1 term		Approximate, 2 terms			
Ta	k_c	Ra_c	k_c	Ra_c	k_c	Ra_c	k_c	Ra_c	k_c	Ra_c
10	3.11	1712.7	3.10	1713.0	3.12	1718.9	3.12	1712.7	7.59	76 860
100	3.13	1756.4	3.15	1756.6	3.15	1753.3	3.16	1754.0	7.60	76 970
500	3.32	1940.2	3.30	1940.5	3.27	1900.6	3.31	1933.0	7.64	77 470
1000	3.48	2151.4	3.50	2151.7	3.41	2074.7	3.48	2137.1	7.68	78 100
2000	3.74	2530.2	3.75	2530.5	3.64	2397.4	3.73	2502.3	7.77	79 320
5000	4.27	3468.5	4.25	3469.2	4.14	3239.8	4.23	3401.6	8.00	82 840
10^4	4.78	4712.1	4.80	4713.1	4.69	4420.6	4.73	4583.3	8.35	88 310
3×10^4	5.79	8324.6	5.80	8326.4	5.87	8078.3	5.69	7994.8	9.35	1.070×10^5
10^5	7.17	1.6720×10^4	7.20	1.6721×10^4	7.56	1.710×10^4	7.10	1.611×10^4	11.2	1.553×10^5
10^6	10.82	7.109×10^4	10.80	7.1132×10^4	11.9	7.857×10^4	11.4	7.393×10^4	17.1	4.702×10^5
10^8	24.64	1.525×10^6	24.5	1.5313×10^6	27.2	1.761×10^6	27.0	1.740×10^6	39.3	8.194×10^6
10^{10}	58.50	3.480×10^7	55.5	3.4636×10^7	59.7	3.912×10^7	59.7	3.903×10^7	95.0	2.555×10^9

$$\tilde{B}_{11} = \frac{\pi^3 k}{(k^2+\pi^2)^3}\left(\frac{8\pi(\cosh k+1)}{(\pi^2+k^2)^2(k+\sinh k)} + \frac{k\coth\frac{k}{2}}{\sinh k - k} - \frac{k+\sinh k}{k(\sinh k - k)} + \frac{4k}{\pi^2+k^2}\right). \quad (27)$$

Curves showing Ra vs. k for several values of Ta as given by (25) are shown in Figure 1. Table I compares the results for the minima of these curves with those found numerically from the exact expression (B7) and those given in Chandrasekhar.[2] The differences between the exact results and those given by the one-term truncation are about 2% for $Ta \le 10^5$. The approximation accuracy degrades considerably for larger Ta with a difference of 15% at $Ta = 10^8$, but the error decreases as Ta increases further until, as shown below, it vanishes as $Ta \to \infty$. The table also includes the results of the present method when two terms, rather than one, are retained in (21). The results are somewhat improved, but the correction is relatively small. In this latter case, the present method also gives a result for the next mode which is shown in the last column.

For the case of free slip at the plates, Chandrasekhar[2] established that, as $Ta \to \infty$, the minimum value Ra_c of Ra and the corresponding wave number k_c are approximately given by

$$Ra_c \simeq \left(\frac{27\pi^4}{4}\right)^{1/3} Ta^{2/3}, \qquad k_c \sim \left(\frac{\pi^2}{2}\right)^{1/6} Ta^{1/6}. \quad (28)$$

It was later shown[3] that these results are also applicable to the no-slip case and it is therefore of interest to compare them with the present ones. We find that, for large k, (23) reduces to

$$Ra \simeq k^4 + \frac{\pi^2}{k^2} Ta. \quad (29)$$

Upon setting the derivative of Ra as given by this relation to 0 we find the same results shown in (28). This is not surprising because, as shown by Chandrasekhar,[2] the results (28) are precisely the consequence of approximating the velocity by its first term in the Fourier series expansion, which is how the approximation (25) was derived. Graphs of Ra_c and k_c vs. Ta as given by the present theory truncated to the first term are provided in Figures 2 and 3, respectively. The dashed-dotted line in the former figure is the exact result for free-slip plates of Ref. 6. It is seen that, while this curve approaches the no-slip results for large Ta, its behavior for smaller Ta is quite different.

In the opposite limit of k small we have

$$\tilde{A}_{11} \simeq \frac{4k^2}{\pi^8}, \qquad \tilde{B}_{11} \simeq \frac{2}{\pi^2}\left(\frac{8}{\pi^2} - \frac{1}{3}\right), \quad (30)$$

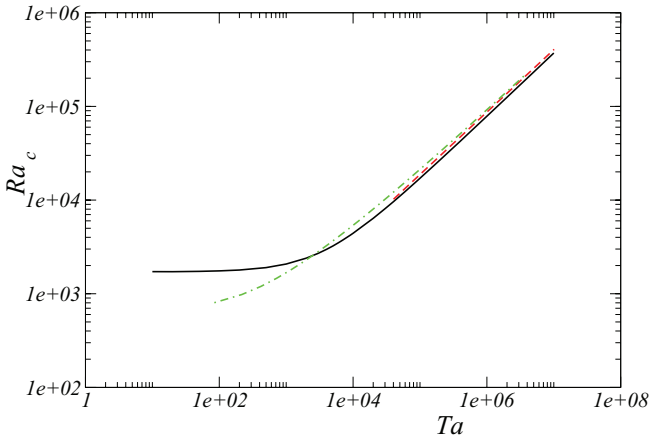

FIG. 2. The critical Rayleigh number vs. the Taylor number for the neutral stability of the even modes with no-slip plates at fixed temperatures (i.e., $\kappa \to \infty$) as given by the present solution truncated to the first term of the Fourier expansion. The dashed line is the large-Ta approximation (28) and the dashed-dotted line is the exact result for free-slip plates of Ref. 6.

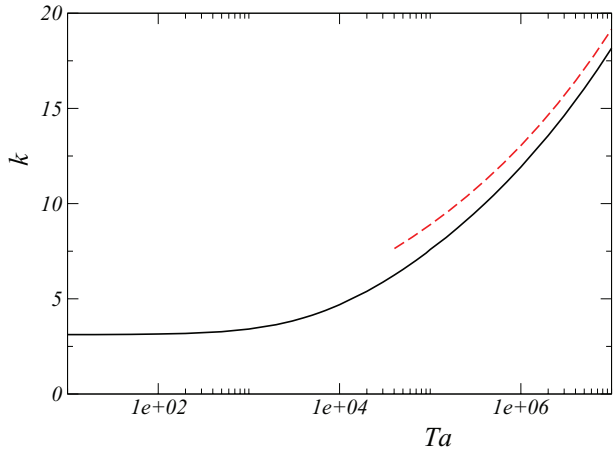

FIG. 3. The critical (dimensionless) wave number vs. the Taylor number for the neutral stability of the even modes with no-slip plates at fixed temperatures (i.e., $\kappa \to \infty$) as given by the present solution truncated to the first term of the Fourier expansion. The dashed line is the large-Ta approximation (28).

so that

$$Ra \simeq \frac{\pi^4 - (15 - \frac{2}{3}\pi^2)Ta}{\pi^2 - 4} \frac{\pi^2}{k^2}. \tag{31}$$

The divergence proportionally to k^{-2} is the same as that encountered in the case with no rotation.[2,11]

A. Variable plate temperature

As mentioned in the Introduction, it is a known fact that the instability ceases to have an oscillatory character when the Prandtl number of the fluid exceeds about 0.68 and the thermal conductivity of the plates is infinite. No such estimates are available for finite thermal conductivities although, by continuity, one would expect the existence of an analogous Prandtl number threshold in this case as well. In this part of our work we proceed heuristically assuming that such a Prandtl number range exists and show some results for finite thermal conductivities.

When the plates have an equal finite thermal conductivity κ, the term

$$\frac{k}{\kappa \coth\frac{k}{2} + 1} \left(\frac{k - \sinh k}{k + \sinh k} \frac{\coth\frac{k}{2}}{k^2} - \frac{1}{k + \sinh k} + \frac{4 \coth\frac{k}{2}}{\tilde{\Delta}_n} \right) \frac{\pi^2}{(\pi^2 + k^2)^3} \tag{32}$$

needs to be subtracted from the expression (26) of $\tilde{A}_{11}$ while the expression (27) of $\tilde{B}_{11}$ remains unchanged. In view of the minus sign in front of $\tilde{A}_{11}$ in the marginal stability condition in (25), this new term increases the left-hand side of (25) and, therefore, lowers the value of Ra for the same Ta and k. Thus, as in the case without rotation,[11,18] a finite plate thermal conductivity destabilizes the system. This feature is demonstrated in Figures 4 and 5 which show the marginal stability curves for $Ta = 10^3$ and $Ta = 10^6$ and different values of the plate thermal conductivity κ. The merging of the curves at large k for high conductivity lends some support to the expectation mentioned earlier that, for sufficiently large Prandtl numbers, the onset of the instability is non-oscillatory also in the case of finite κ.

A new feature that is introduced by a finite plate thermal conductivity, and which is also encountered in the case without rotation, is a modification of the functional dependence of Ra on the wave number k for small k. Now the leading-order behavior of $\tilde{A}_{11}$ for $k \to 0$ is

$$\tilde{A}_{11} \simeq \frac{2}{\pi^4} \left(\frac{4}{\pi^2} - \frac{1}{3} \right) \frac{k}{2\kappa + k}. \tag{33}$$

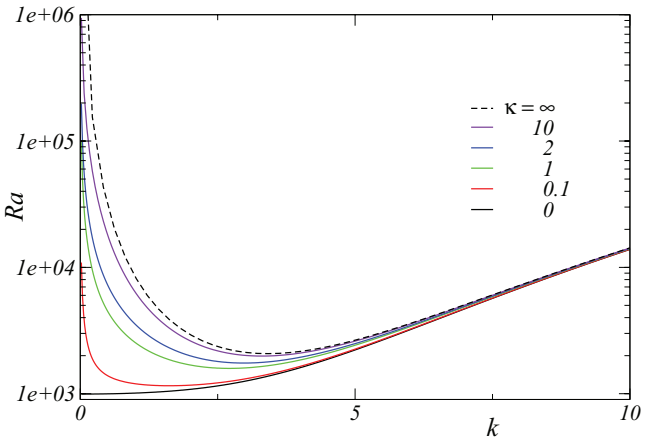

FIG. 4. The Rayleigh number for the neutral stability of the even modes for $Ta = 10^3$ and different plate thermal conductivities; in ascending order $\kappa = 0$ (i.e., thermally insulating plates), 0.1, 1, 2, and 10. The topmost dashed line is for $\kappa \to \infty$, namely, for fixed plate temperature and is the same line shown in Figure 1. The fluid velocity vanishes at the plates.

For perfectly insulating plates ($\kappa = 0$) and small k, the critical Rayleigh number tends to the constant

$$Ra \simeq \frac{3\pi^6 + (5\pi^2 - 48)Ta}{2(12 - \pi^2)}, \tag{34}$$

as evident in Figures 4 and 5. On the other hand, if $\kappa \neq 0$, to leading order Ra diverges as k^{-1} for $k \to 0$,

$$Ra \simeq \frac{3\pi^6 + (5\pi^2 - 48)Ta}{12 - \pi^2} \frac{\kappa}{k}. \tag{35}$$

In the opposite limit of large k all the curves merge together and the finite thermal conductivity of the plates quickly becomes immaterial.

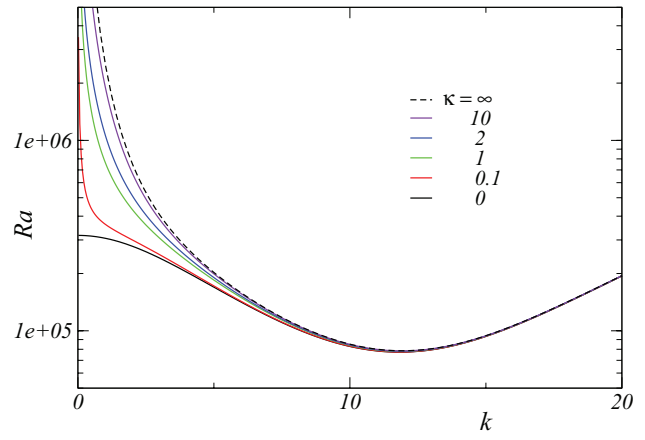

FIG. 5. The Rayleigh number for the neutral stability of the even modes for $Ta = 10^6$ and different plate thermal conductivities; in ascending order $\kappa = 0$ (i.e., thermally insulating plates), 0.1, 1, 2, and 10. The topmost dashed line is for $\kappa \to \infty$, namely, for fixed plate temperature and is the same line shown in Figure 1. The fluid velocity vanishes at the plates.

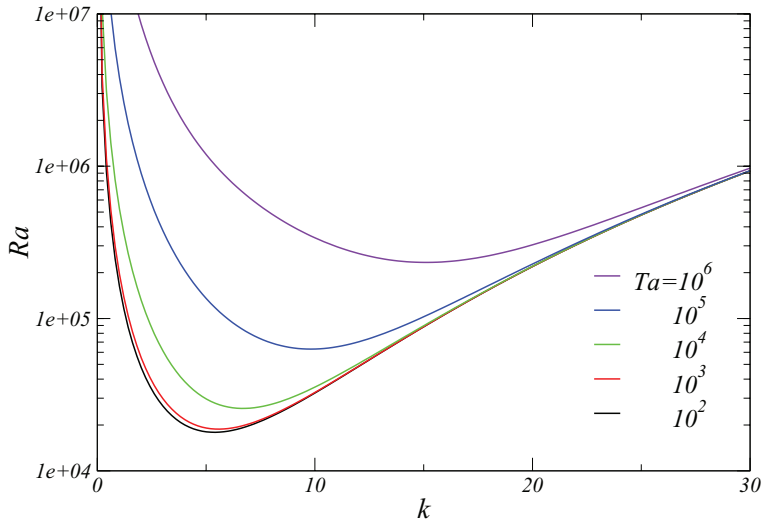

FIG. 6. The Rayleigh number for the neutral stability of the odd modes as given by the present solution truncated to the first term of the Fourier expansion. The no-slip condition is applied at the plates, which are assumed to be infinitely conducting so that $\kappa \to \infty$ and their temperatures is fixed. In ascending order $Ta = 10^2$, 10^3, 10^4, 10^5, and 10^6.

VI. ODD MODES

Marginal stability curves for the odd modes as given by the present theory (24) for fixed plate temperatures and a one-term truncation are shown in Figure 6 for several values of the Taylor number. In this case there do not seem to be exact results available.

Numerical results for the minima of these curves are given in Table II for a one-term truncation (second column) and a two-term truncation. For this latter case the present method also gives the next mode, the results for which are shown in the last pair of columns.

TABLE II. The smallest Rayleigh number and corresponding dimensionless wave number for the marginal stability threshold of the odd modes as functions of the Taylor number, shown in the first column, according to the present approximate solution. The no-slip condition is applied at the plates, which are assumed to be infinitely conducting so that $\kappa \to \infty$ and their temperatures are fixed. The second and third columns are for the lowest odd mode and a one-term truncation of the Fourier series, Eq. (24). The third and fourth columns are also for the lowest odd mode but with a two-term truncation. In this latter case, the present method also gives a result for the next mode which is shown in the last two columns.

	Present, 1 term		Present, 2 terms			
Ta	k_c	Ra_c	k_c	Ra_c	k_c	Ra_c
10	5.366	17 813.41	5.366	17 632.86	9.825	223 652.88
100	5.386	17 904.60	5.388	17 732.46	9.829	223 779.10
500	5.472	18 301.89	5.480	18 165.35	9.847	224 338.87
1000	5.570	18 781.88	5.586	18 686.23	9.870	225 035.84
2000	5.747	19 694.76	5.776	19 671.18	9.914	226 420.79
5000	6.174	22 157.30	6.225	22 297.56	10.042	230 506.81
10^4	6.692	25 684.04	6.759	25 999.81	10.244	237 105.47
2×10^4	7.402	31 580.90	7.474	32 080.44	10.607	249 620.90
5×10^4	8.644	45 312.68	8.686	45 915.10	11.481	283 156.55
10^5	9.810	62 980.00	9.791	63 370.78	12.534	330 672.04
10^6	15.102	23 3471.61	14.869	229 678.175	18.638	815 617.161
10^8	34.357	4 612 176.25	34.202	4 578 836.23	43.059	12 438 660.5
10^{10}	75.405	99 724 723.7	75.345	99 574 812.8	94.987	255 543 249.

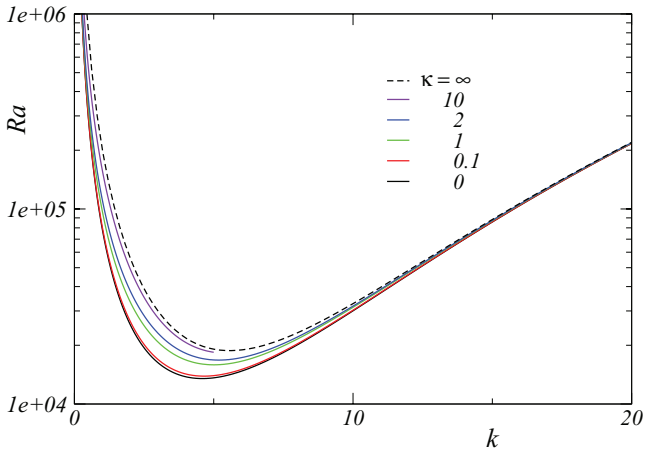

FIG. 7. The Rayleigh number for the neutral stability of the odd modes for $Ta = 10^3$ and different plate thermal conductivities; in ascending order $\kappa = 0$ (i.e., thermally insulated plates), 0.1, 1, 2, and 10. The topmost dashed line is for $\kappa \to \infty$, namely, for fixed plate temperature and is the same line shown in Figure 6. The fluid velocity vanishes at the plates.

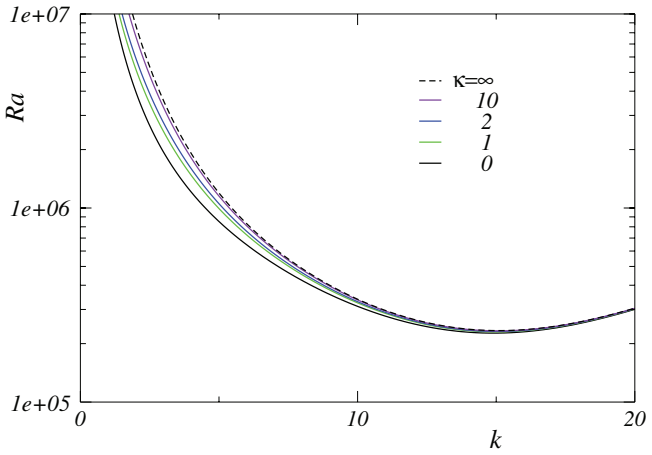

FIG. 8. The Rayleigh number for the neutral stability of the odd modes for $Ta = 10^6$ and different plate thermal conductivities; in ascending order $\kappa = 0$ (i.e., thermally insulated plates), 1, 2, and 10. The topmost dashed line is for $\kappa \to \infty$, namely, for fixed plate temperature and is the same line shown in Figure 6. The fluid velocity vanishes at the plates.

The effect of a finite plate thermal conductivity is shown in Figures 7 and 8. If $\kappa \neq 0$ the threshold value of the Rayleigh number becomes infinite for both small and large k. As before, the curves merge as k increases irrespective of the value of the thermal conductivity.

VII. CONCLUSIONS

By solving the Rayleigh-Bénard linear marginal stability problem by a strategy somewhat different from the standard one, we have found relatively simple explicit analytical approximations for the dependence of the Rayleigh number on the Taylor number Ta and the wave number k. Where the results can be compared with more precise ones, it is found that the error is of the order of a few percent over most of the range of Ta and k.

The results confirm much that is already known: the most unstable modes are even with respect to the midplane between the two plates, and the critical value of the Rayleigh number has a minimum Ra_c in correspondence with a wave number k_c which increases as the Taylor number increases. A new result concerns the effects of a finite thermal conductivity of the solid boundaries, which is

found to be destabilizing as in the case without rotation. Furthermore, the relative simplicity of the approximate result has allowed us to calculate the dependence of Ra on k and Ta in a straightforward way.

While the present results refer to the linear threshold problem and are only approximate, their good accuracy makes them useful to gain a quick understanding of the system behavior. Furthermore, it appears that the same method might be useful to explore other aspects of the problem: finite plate thickness, convection in a porous medium, overstability and perhaps time-dependent processes.

APPENDIX A: ALGEBRAIC DETAILS

We give here some additional details on the calculations summarized in Sec. III. A detailed derivation is provided in the supplementary material.[17]

We start by showing the explicit expressions of the functions $G_{c,\,s}$ and $H_{c,\,s}$ introduced in (16):

$$G_c = \frac{z}{2k}\sinh kz, \qquad G_s = \frac{z}{2k}\cosh kz, \tag{A1}$$

$$H_c = \frac{z}{8k^2}\left(-\frac{\sinh kz}{k} + z\cosh kz\right), \qquad H_s = \frac{z}{8k^2}\left(-\frac{\cosh kz}{k} + z\sinh kz\right). \tag{A2}$$

These are, respectively, particular solutions of $(\partial_z^2 - k^2)G_{c,s} = F_{c,s}$ and $(\partial_z^2 - k^2)^2 H_{c,s} = F_{c,s}$ with $F_{c,\,s}$ given in (15).

Upon imposing that u_z' and $\partial_z u_z'$ as given by (16) and its derivative vanish on the plates $z = \pm\frac{1}{2}$ we can express the integration constants $U_{c,\,s}$ and $V_{c,s}$ in terms of $W_{c,s}$. The results are

$$U_c = -\frac{\sinh\frac{k}{2}}{k+\sinh k}\sum_{m=1}^{\infty}\frac{(-1)^{m+1}(2m-1)\pi}{\tilde\Delta_m^2}\left(\frac{(Ra+Ta)k^2}{\tilde\Delta_m} - Ta\right)\tilde U_m + \frac{\sinh k - k}{\sinh k + k}\frac{W_c}{32k^2}, \tag{A3}$$

$$V_c = \frac{4k\cosh\frac{k}{2}}{\sinh k + k}\sum_{m=1}^{\infty}\frac{(-1)^{m+1}(2m-1)\pi}{\tilde\Delta_m^2}\left(\frac{(Ra+Ta)k^2}{\tilde\Delta_m} - Ta\right)\tilde U_m + \frac{\sinh k - k\cosh k}{\sinh k + k}\frac{W_c}{4k^2}, \tag{A4}$$

and

$$U_s = -\frac{\cosh\frac{k}{2}}{\sinh k - k}\sum_{m=1}^{\infty}\frac{2(-1)^{m+1}m\pi}{\Delta_m^2}\left(\frac{(Ra+Ta)k^2}{\Delta_m} - Ta\right)U_m + \frac{\sinh k + k}{\sinh k - k}\frac{W_s}{32k^2}, \tag{A5}$$

$$V_s = \frac{4k\sinh\frac{k}{2}}{\sinh k - k}\sum_{m=1}^{\infty}\frac{2(-1)^{m+1}m\pi}{\Delta_m^2}\left(\frac{(Ra+Ta)k^2}{\Delta_m} - Ta\right)U_m + \frac{\sinh k - k\cosh k}{\sinh k - k}\frac{W_s}{4k^2} \tag{A6}$$

with Δ_m and $\tilde\Delta_m$ defined in (14).

It remains to calculate the constants $W_{c,s}$. To this end we impose that the momentum equation in the form (3) be satisfied at the plate surfaces. For this purpose it is necessary to solve (1) and (2) to express the temperature and vorticity perturbations in terms of u_z'. This task is readily accomplished in terms of a suitable Green's function (or by the method of variation of parameters) and, after imposing the vanishing of ω_z' at the plate surfaces and the boundary conditions (10) on T', we find

$$\omega_z' = -\sqrt{Ta}\int_{-1/2}^{z} u_z'(\zeta)\,\cosh k(z-\zeta)\,d\zeta + \sqrt{Ta}\frac{\sinh k(z+\frac{1}{2})}{\sinh k}I_C \tag{A7}$$

and

$$T' = -\frac{Pr}{k}\int_{-1/2}^{z} u_z'(\zeta)\,\sinh k(z-\zeta)\,d\zeta + \Theta_c F_c + \Theta_s F_s \tag{A8}$$

with

$$k\left[(\kappa_l+\kappa_u)\cosh k+(1+\kappa_l\kappa_u)\sinh k\right]\Theta_c \;=\; Pr\left(\kappa_l\sinh\frac{k}{2}+\cosh\frac{k}{2}\right)\left[\kappa_u I_S+I_C\right], \tag{A9}$$

$$k\left[(\kappa_l+\kappa_u)\cosh k+(1+\kappa_l\kappa_u)\sinh k\right]\Theta_s \;=\; Pr\left(\kappa_l\cosh\frac{k}{2}+\sinh\frac{k}{2}\right)\left[\kappa_u I_S+I_C\right], \tag{A10}$$

in which

$$I_S \;=\; \int_{-1/2}^{1/2} u_z'(\zeta)\,\sinh k(\tfrac{1}{2}-\zeta)\,d\zeta, \qquad I_C \;=\; \int_{-1/2}^{1/2} u_z'(\zeta)\,\cosh k(\zeta-\tfrac{1}{2})\,d\zeta. \tag{A11}$$

It may be noted that, in the steps that follow, the Prandtl number in (A9) and (A10) combines with the Grashof number to give the Rayleigh number, $Ra = GrPr$. Thus, when the instability onset is non-oscillatory as assumed here, the marginal stability condition ends up depending only on Ra rather than on both Ra and Pr.

The expressions (A9) and (A10) for $\Theta_{c,\,s}$, which are a consequence of the boundary conditions (10), simplify when the plate thermal conductivities are equal, $\kappa_l = \kappa_u = \kappa$,

$$k\left(\kappa\cosh\frac{k}{2}+\sinh\frac{k}{2}\right)\Theta_c \;=\; Pr\left[\kappa I_S+I_C\right], \tag{A12}$$

$$k\left(\kappa\sinh\frac{k}{2}+\cosh\frac{k}{2}\right)\Theta_s \;=\; Pr\left[\kappa I_S+I_C\right]. \tag{A13}$$

This is the case that we have considered in the paper and that we consider henceforth. The significant simplification stems from the fact that, with equal plate thermal conductivity, the modes maintain a definite parity, which is lost if $\kappa_l \neq \kappa_u$ as shown for the non-rotating case, e.g., in Ref. 11.

Upon substituting (A8) and the derivative of (A7) into the momentum equation (3) and evaluating at $z = \pm\frac{1}{2}$ we determine $W_{c,s}$,

$$W_c \;=\; k\left[\frac{Ta}{\sinh k}+\frac{Ra}{\kappa(\cosh k+1)+\sinh k}\right]J_C, \tag{A14}$$

$$W_s \;=\; k\left[\frac{Ta}{\sinh k}+\frac{Ra}{\kappa(\cosh k-1)+\sinh k}\right]J_S, \tag{A15}$$

in which

$$J_C \;=\; \int_{-1/2}^{1/2} u_z'\cosh kz\,dz \;=\; -2\pi\cosh\frac{k}{2}\sum_{m=1}^{\infty}\frac{(2m-1)(-1)^m}{\tilde\Delta_m}\tilde U_m, \tag{A16}$$

$$J_S \;=\; \int_{-1/2}^{1/2} u_z'\sinh kz\,dz \;=\; -2\pi\sinh\frac{k}{2}\sum_{m=1}^{\infty}\frac{2m\pi(-1)^m}{\Delta_m}U_m. \tag{A17}$$

Upon substitution of the expression for W_s in the right-hand side of (17) we form the right-hand side of (20) in which

$$A_{nm} \;=\; \frac{2(-1)^{m+1}m\pi}{\Delta_m}\left(\frac{k^2\alpha_n}{\Delta_m^2}-\frac{k\beta_n}{\kappa\tanh\frac{k}{2}+1}\right), \tag{A18}$$

$$B_{nm} \;=\; \frac{2(-1)^{m+1}m\pi}{\Delta_m}\left(\frac{(2\pi m)^2\alpha_n}{\Delta_m^2}+k\beta_n\right) \tag{A19}$$

with

$$\alpha_n = \frac{16(-1)^{n+1}\pi nk(\cosh k - 1)}{\Delta_n^2(\sinh k - k)}, \tag{A20}$$

$$\beta_n = \frac{2(-1)^{n+1}\pi n}{\Delta_n^2}\left[\frac{1}{\sinh k - k} - \frac{k + \sinh k}{\sinh k - k}\frac{\tanh\frac{k}{2}}{k^2} + \frac{4\tanh\frac{k}{2}}{\Delta_n}\right]. \tag{A21}$$

Similarly, upon substitution of the expression for W_c in the right-hand side of (18), we form the right-hand side of (21) in which

$$\tilde{A}_{nm} = \frac{(-1)^{m+1}(2m-1)\pi}{\tilde{\Delta}_m}\left(\frac{k^2\tilde{\alpha}_n}{\tilde{\Delta}_m^2} - \frac{k\tilde{\beta}_n}{\kappa\coth\frac{k}{2} + 1}\right), \tag{A22}$$

$$\tilde{B}_{nm} = \frac{(-1)^{m+1}(2m-1)\pi}{\tilde{\Delta}_m}\left(\frac{(2m-1)^2\pi^2\tilde{\alpha}_n}{\tilde{\Delta}_m^2} + k\tilde{\beta}_n\right) \tag{A23}$$

with

$$\tilde{\alpha}_n = \frac{8(-1)^{n+1}(2n-1)\pi k(\cosh k + 1)}{\tilde{\Delta}_n^2(k + \sinh k)}, \tag{A24}$$

$$\tilde{\beta}_n = \frac{(-1)^{n+1}(2n-1)\pi}{\tilde{\Delta}_n^2}\left(\frac{k - \sinh k}{k + \sinh k}\frac{\coth\frac{k}{2}}{k^2} - \frac{1}{k + \sinh k} + \frac{4\coth\frac{k}{2}}{\tilde{\Delta}_n}\right). \tag{A25}$$

APPENDIX B: DIRECT EXACT SOLUTION

We develop here the equation for marginal stability according to the standard procedure,[2,3] as the result given in the latter reference contains some misprints. This approach is more direct that the one followed before, but it leads to a much more involved expression which is not easily evaluated. We only consider the case with fixed plate temperatures for simplicity but, unlike Ref. 3, we also give the result for modes with an odd parity.

After elimination of the temperature and vorticity perturbations the momentum equation (3) becomes

$$(\partial_z^2 - k^2)^3 u_z' + Rak^2 u_z' + Ta\partial_z^2 u_z' = 0. \tag{B1}$$

Upon looking for solutions in the form of superpositions of terms proportional to $e^{i\lambda z}$ we find the characteristic equation which is conveniently written as

$$(\lambda^2 + k^2)^3 + Ta(\lambda^2 + k^2) - k^2(Ra + Ta) = 0. \tag{B2}$$

It is easily seen that this cubic equation in λ^2 has one real non-negative solution λ_1^2 and two complex conjugate solutions $\lambda_{2,3}^2$.

The lowest mode is even and, therefore, we write

$$u_z' = \sum_{j=1}^{3}\tilde{A}_j\cos\lambda_j z. \tag{B3}$$

The vanishing of u_z' and $\partial_z u_z'$ at $z = \pm\frac{1}{2}$ give

$$\sum_{j=1}^{3}\tilde{A}_j\cos\frac{\lambda_j}{2} = 0, \qquad \sum_{j=1}^{3}\tilde{A}_j\lambda_j\sin\frac{\lambda_j}{2} = 0. \tag{B4}$$

The vorticity is readily find by integrating (2) and imposing vanishing boundary conditions at $z = \pm\frac{1}{2}$,

$$\omega_z' = -\sqrt{Ta}\sum_{j=1}^{3}\frac{\lambda_j}{\lambda_j^2+k^2}\tilde{A}_j\sin\lambda_j z + \sqrt{Ta}\frac{\sinh kz}{\sinh\frac{k}{2}}\sum_{j=1}^{3}\frac{\lambda_j}{\lambda_j^2+k^2}\tilde{A}_j\sin\frac{\lambda_j}{2}. \tag{B5}$$

Upon demanding that the momentum equation in the form (3) be satisfied at $z = \pm\frac{1}{2}$, with the aid of (B2), we are led to

$$k\,Ta\,\coth\frac{k}{2}\sum_{j=1}^{3}\left[\frac{k\,(Ra/Ta)\tanh\frac{k}{2}-\lambda_j\tan\frac{\lambda_j}{2}}{\lambda_j^2+k^2}\right]\tilde{A}_j\cos\frac{\lambda_j}{2} = 0. \tag{B6}$$

The requirement that the determinant of the algebraic system (B4) and (B6) vanish leads us to

$$\mathrm{Im}\left\{\frac{(\gamma_1-\gamma)\gamma_2}{\lambda_1^2+k^2}-\frac{(\gamma_2-\gamma)(\gamma_1-\overline{\gamma}_2)}{\lambda_2^2+k^2}\right\} = 0, \tag{B7}$$

where the overline denotes the complex conjugate and we have adopted the notation of Ref. 3:

$$\gamma_j = \lambda_j\tan\frac{\lambda_j}{2}, \qquad \gamma = \frac{Ra}{Ta}\,k\,\tanh\frac{k}{2}. \tag{B8}$$

Equation (B7) establishes a connection among k, Ta, and Ra at marginal stability conditions. For a given value of Ta, the curve expressing Ra as a function of k has a minimum $Ra = Ra_c$ for $k = k_c$. The numerical values shown in Table I have been found iteratively by following the gradient of the function in the left-hand side of (B7) with respect to the variables k and Ra. The derivatives have been computed numerically and under-relaxation was applied with respect to k.

For the odd modes we proceed similarly starting from

$$u_z' = \sum_{j=1}^{3}A_j\sin\lambda_j z, \tag{B9}$$

and, in place of (B4), find

$$\sum_{j=1}^{3}A_j\sin\frac{\lambda_j}{2} = 0, \qquad \sum_{j=1}^{3}A_j\lambda_j\cos\frac{\lambda_j}{2} = 0. \tag{B10}$$

The vorticity is now given by

$$\omega_z' = \sqrt{Ta}\sum_{k=1}^{3}\frac{\lambda_k}{\lambda_k^2+k^2}A_k\cos\lambda_k z - \sqrt{Ta}\,\frac{\cosh kz}{\cosh\frac{k}{2}}\sum_{k=1}^{3}\frac{\lambda_k}{\lambda_k^2+k^2}A_k\cos\frac{1}{2}\lambda_k \tag{B11}$$

and the analog of (B6) follows as before in the form to

$$k\,Ta\,\tanh\frac{k}{2}\sum_{k=1}^{3}\left[\frac{k\,(Ra/Ta)\coth\frac{k}{2}-\lambda_k\cot\frac{1}{2}\lambda_k}{\lambda_k^2+k^2}\right]A_k\sin\frac{1}{2}\lambda_k = 0. \tag{B12}$$

If we now set

$$\gamma_k = \lambda_k\cot\frac{1}{2}\lambda_k, \qquad \gamma = \frac{Ra}{Ta}\,k\,\coth\frac{k}{2}, \tag{B13}$$

the marginal stability condition retains the form (B7) of the previous case.

[1] S. Chandrasekhar, "The instability of a layer of fluid heated below and subject to Coriolis forces," Proc. R. Soc. London, Ser. A **217**, 306 (1953).
[2] S. Chandrasekhar, *Hydrodynamic and Hydromagnetic Stability* (Clarendon, Oxford, 1961), reprinted by Dover, New York, 1981.
[3] P. P. Niiler and F. E. Bisshopp, "On the influence of Coriolis force on onset of thermal convection," J. Fluid Mech. **22**, 753 (1965).

[4] G. M. Homsy and J. L. Hudson, "The asymptotic stability of a bounded rotating fluid heated from below: conductive basic state," J. Fluid Mech. **45**, 353 (1971).
[5] K. Zhang and P. H. Roberts, "Thermal inertial waves in a rotating fluid layer: Exact and asymptotic solutions," Phys. Fluids **9**, 1980 (1997).
[6] R. C. Kloosterziel and G. F. Carnevale, "Closed-form linear stability conditions for rotating Rayleigh-Bénard convection with rigid stress-free upper and lower boundaries," J. Fluid Mech. **480**, 25 (2003).
[7] R. M. Clever and F. H. Busse, "Nonlinear properties of convection rolls in a horizontal layer rotating about a vertical axis," J. Fluid Mech. **94**, 9 (1979).
[8] H. F. Goldstein, E. Knobloch, I. Mercader, and M. Net, "Convection in a rotating cylinder. Part 2. Linear theory for low Prandtl numbers," J. Fluid Mech. **262**, 293 (1994).
[9] J. H. P. Dawes, "Rapidly rotating thermal convection at low Prandtl number," J. Fluid Mech. **428**, 61 (2001).
[10] B. A. Finlayson, "The Galerkin method applied to convective instability problems," J. Fluid Mech. **33**, 201 (1968).
[11] A. Prosperetti, "A simple analytic approximation to the Rayleigh-Bénard stability threshold," Phys. Fluids **23**, 124101 (2011).
[12] N. D. Stein, "Exact sine series solution for oscillatory convection in a binary fluid," Phys. Rev. A **43**, 768 (1991).
[13] M. R. Ardron, P. G. J. Lucas, and N. D. Stein, "Exact calculation of convection thresholds in rotating binary liquid mixtures," Phys. Fluids A **4**, 664 (1992).
[14] E. Bodenschatz, W. Pesch, and G. Ahlers, "Recent developments in Rayleigh-Bénard convection," Annu. Rev. Fluid Mech. **32**, 709 (2010).
[15] G. Ahlers, S. Grossmann, and D. Lohse, "Heat transfer and large scale dynamics in turbulent Rayleigh-Bénard convection," Rev. Mod. Phys. **81**, 503 (2009).
[16] D. Lohse and K.-Q. Xia, "Small-scale properties of turbulent Rayleigh-Bénard convection," Annu. Rev. Fluid Mech. **42**, 335 (2010).
[17] See supplementary material at http://dx.doi.org/10.1063/1.4764931 for a detailed derivation of the results of Appendix A.
[18] D. A. Nield, "The Rayleigh-Jeffreys problem with boundary slab of finite conductivity," J. Fluid Mech. **32**, 393 (1968).
[19] The problem studied in a recent paper by P. Falsaperla and G. Mulone ("Stability in the rotating Bénard problem with Newton-Robin and heat fixed flux boundary conditions," Mech. Res. Commun. **37**, 122 (2010)) is only superficially similar to the present one. These authors write Newton-Robin conditions in a generic *a priori* form rather than deriving them from the physical consideration of heat conduction in the bounding plates as done here. The consequence is that their boundary conditions, analogous to those shown in (10), are not dependent on the wave number. Given the crucial role played by the wave number in the entire theory, this is a major difference that makes their results irrelevant in the present context.